© 2015. Published by The Company of Biologists Ltd | Development (2015) 142, 883-892 doi:10.1242/dev.113902

RESEARCH ARTICLE

STEM CELLS AND REGENERATION

Activin signaling balances proliferation and differentiation of ovarian niche precursors and enables adjustment of niche numbers

Tamar Lengil*, Dana Gancz* and Lilach Gilboa‡

ABSTRACT

How the numbers of niches and resident stem cells within a particular organ are determined during development and how they may be modulated or corrected is a question with significant medical implications. In the larval ovary of *Drosophila melanogaster*, somatic precursors for niches, and germ cells that will become germline stem cells, co-develop. Somatic precursors proliferate during the first 3 days of larval development. By mid-third instar, adult terminal filament (TF) (part of the germline stem cell niche) cells first appear, and differentiation terminates 24 h later when 16-20 TFs fully form. The developmental sequence responsible for TF cell determination and final TF numbers is only partially understood. We show that TF formation proceeds through several, hitherto uncharacterized stages, which include an early exit from the cell cycle to form TF precursors and two steps of cell shape change to form the mature TF cells. The Activin receptor Baboon (Babo) is required for somatic precursor cell proliferation and therefore determines the pool of TF precursors available for TF differentiation. During the final differentiation stage, Babo facilitates TF and germ cell differentiation, and promotes the accumulation of Broad-Z1, which is also a target of the steroid hormone ecdysone. Epistasis analysis shows that Activin controls cell proliferation in an ecdysone-independent manner and TF differentiation by affecting ecdysone targets. We propose that this mode of function allows Activin to balance proliferation and differentiation, and to equilibrate niche numbers. These results suggest a novel model for how niche numbers are corrected during development.

KEY WORDS: *Drosophila*, Niche, Ovary, Activin, Ecdysone, Germline stem cells

INTRODUCTION

Stem cells and their niches constitute functional units that support organ homeostasis and regeneration. How stem cell unit numbers are determined during development remains an open question (O'Brien and Bilder, 2013). In the ovary of *Drosophila melanogaster*, 16-20 stem cell units form during larval development. These units are composed of somatic terminal filament (TF), escort and cap cells, which attach to two or three germline stem cells (GSCs) (Chen et al., 2011; Eliazer and Buszczak, 2011; Losick et al., 2011; Spradling et al., 2011). Both the somatic and germline components of the GSC unit originate from precursor cells. During the first 4 days after egg laying (AEL; for timing of larval development see Materials and Methods), primordial germ cells (PGCs, the precursors of GSCs) and the somatic precursors proliferate (Fig. 1A). At mid-third larval instar (ML3, 96 h AEL), cells that are positive for TF markers first appear (Gancz et al., 2011; Godt and Laski, 1995; Sahut-Barnola et al., 1995; Zhu and Xie, 2003). During the last day of larval development (96-120 h AEL), TFs gradually form, a process that occurs simultaneously with somatic precursor cell proliferation. Once formed, TFs induce cap cell formation by Notch signaling (Song et al., 2007). PGCs then attach to the cap cells via E-Cadherin (Shotgun – FlyBase) to form the completed stem cell unit (Song et al., 2002).

Previous work identified several transcription factors and signaling pathways that contribute to TF formation and numbers, including Engrailed (En), Bric a brac and Pipsqueak (Bartoletti et al., 2012; Bolivar et al., 2006; Godt and Laski, 1995; Sahut-Barnola et al., 1995). Nutritional cues, such as the Insulin and Tor pathways, also affect TF numbers (Gancz and Gilboa, 2013b; Green and Extavour, 2012, 2014; Sarikaya et al., 2012).

Ecdysone is another hormonal cue that promotes TF formation (Gancz and Gilboa, 2013a; Gancz et al., 2011; Hodin and Riddiford, 1998; Konig et al., 2011). At early larval stages, ecdysone receptors act as repressors of TF differentiation, whereas in the second part of the third instar they become activators of TF differentiation. Ecdysone receptors thus act as a switch between the proliferation of somatic precursor cells and TF differentiation (Gancz et al., 2011). One known ecdysone target that is upregulated at the latter half of the third instar is the zinc-finger and BTB domain transcription factor Broad (Br) (Chao and Guild, 1986; Karim et al., 1993). The *broad* locus encodes four isoforms (Bayer et al., 1996; DiBello et al., 1991), and the Br-Z1 isoform is specifically upregulated in ovarian somatic cells following ecdysone activity (Gancz et al., 2011).

Since Br-Z1 plays a central role in GSC unit formation, it might also provide a hub for controlling the proliferation and differentiation processes that create them. Our present data show that such control occurs through Activin signaling. In *Drosophila*, Activin signaling is transmitted by Baboon (Babo), a type I receptor of the TGF-β superfamily (Massague, 2012; Miyazono et al., 2000). Babo phosphorylates the R-Smad Smox (Smad on X), which, together with the Smad4 homolog Medea, translocates to the nucleus and represses or activates various target genes (Brummel et al., 1999). Activin has been associated with proliferation, differentiation and morphogenetic events occurring in the nervous system, immune system, muscle and during imaginal disc development (Bai et al., 2013; Brummel et al., 1999; Clark et al., 2011; Ellis et al., 2010; Ng, 2008; Parker et al., 2006; Peterson and O'Connor, 2013; Ting et al., 2014; Yu et al., 2013; Zheng et al.,

Department of Biological regulation, Weizmann Institute of Science, Rehovot 76100, Israel.
*These authors contributed equally to this work

‡Author for correspondence (lilach.gilboa@weizmann.ac.il)

Received 5 June 2014; Accepted 23 December 2014

Development (2015) 142, 883-892 doi:10.1242/dev.113902

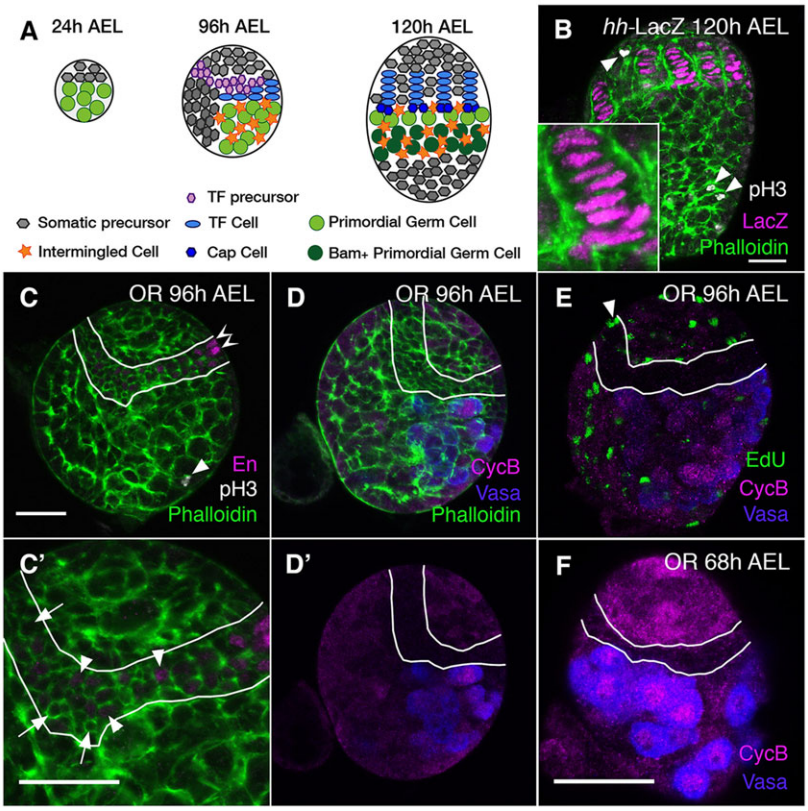

Fig. 1. Reduced proliferation of niche precursors prior to terminal differentiation. (A) Gonad development during *Drosophila* larval stages. Cell types are marked. See text for details. (B-D) Phalloidin (green) marks somatic cell cortices. (B,C) Mitotic cells are labeled by anti-pH3 (white). TF cells are marked either with anti-En or with anti-β-gal (magenta). (B) *hh-lacZ* ovaries at the end of larval development. TF stacks are fully formed (inset). Arrowheads mark mitotic cells. *n*=27 ovaries, containing ~450 TFs. (C) Oregon R (OR) wild type (WT). White lines surround the TF region. Within these lines mature lens-shaped cells (C, chevrons), smaller cells expressing En (C′, arrowheads) and cells devoid of En (C′, arrows) are marked. *n*=46 ovaries. (D-E) Anti-Vasa (blue) stains PGCs and anti-CycB (magenta) stains mitotic cells. TF regions are within white lines. (D,D′) WT ovaries at 96 h AEL. CycB staining is reduced within the TF region. *n*=40 ovaries. (E) EdU (green) labeling of 96 h AEL ovaries. EdU-positive cells are absent from the TF region, but can sometimes be observed at its borders (arrowhead). *n*=17 ovaries. (F) WT ovaries at 68 h AEL. A narrow band of CycB-negative cells is present. *n*=18 ovaries. Scale bars: 20 µm (in C for C,D,D′,E).

2003; Zhu et al., 2008). Activin signaling also acts systemically to control metamorphosis by promoting the expression of several ecdysone biosynthetic enzymes (Gibbens et al., 2011). Interestingly, Activin interacts with the ecdysone pathway also in the nervous system, where it promotes the expression of the ecdysone receptor EcR-B1 in mushroom body γ-neurons, thus potentiating their response to ecdysone (Yu et al., 2013; Zheng et al., 2003).

Our work now uncovers a third mode of interaction between the ecdysone and Activin pathways. We show that Activin is required in the somatic cells of larval ovaries for the correct accumulation of Br-Z1 following ecdysone receptor activation. In addition, Activin promotes somatic precursor cell proliferation independently of ecdysone. Thus, Activin signaling acts as a coordinator of proliferation and differentiation and balances these two opposing forces.

RESULTS

Accumulation of niche precursors during the second and third instars

One of the attributes of TF cells is their inability to self-renew during adulthood (Xie and Spradling, 2000). Indeed, BrdU feeding and mosaic analysis experiments revealed that progeny of proliferating cells could be incorporated into TFs from the end of second larval instar until ~105 h AEL with decreasing efficiency (Godt and Laski, 1995; Sahut-Barnola et al., 1996). To understand how proliferation and differentiation of somatic precursors may modulate niche numbers, we monitored somatic cell proliferation at different times during larval development. We used anti-β-gal or anti-En antibodies to mark TF cells of *hh-lacZ* and Oregon Red (OR) wild-type (WT) flies, respectively; Alexa 488-phalloidin delineated cell shape and anti-phospho-Histone 3 (pH3) detected mitotic cells. At the end of third instar (120 h AEL), pH3-positive cells were observed throughout the organ (Fig. 1B, arrowheads), but not in TF cells, which were stacked in filaments (Fig. 1B, inset).

We next examined whether TF cells could proliferate prior to their stacking in a filament. At 96 h AEL, TF stacking has only just begun, and En-positive cells that were not in stacks could be analyzed (Gancz et al., 2011; Godt and Laski, 1995; Sahut-Barnola et al., 1995). None of these cells was pH3 positive (Fig. 1C,C′). Therefore, TF cells cease proliferating prior to their stacking in filaments.

Interestingly, at 96 h AEL, the region where TFs were forming contained three groups of cells that were shaped differently to other anterior cells (Fig. 1C,C′, between white lines; supplementary material Movie 1). The first group consisted of mature, disc-shaped cells expressing the TF marker En (Fig. 1C, chevrons). Cells in the second group also expressed TF markers, but were cuboidal or box-shaped (Fig. 1C′, arrowheads). The majority of cells in this region belonged to the third group, with the same box-shape but without En expression (Fig. 1C′, arrows). We hypothesize that these three groups might represent a sequence of TF cell formation, whereby cells at the TF region first change their shape, then gain TF marker expression, followed by stacking into filaments and a second shape change to mature disc-like cells.

To determine the proliferation status of the different cells in the TF region, we used antibodies directed against mitotic Cyclin B (CycB). In line with gonad growth at 96 h AEL, many gonadal cells expressed CycB. Strikingly, a band in the region where TF cells formed showed a marked reduction in CycB expression (Fig. 1D,E, between white lines). This suggests that cells in the TF region reduce their proliferation or exit the cell cycle entirely prior to acquiring TF markers. To support this conclusion, we also analyzed EdU incorporation, which marks cells undergoing S phase. The TF region mostly lacked EdU-labeled cells. The few EdU-positive cells

Development (2015) 142, 883-892 doi:10.1242/dev.113902

that were observed in the CycB-reduced region were located at its periphery (Fig. 1E, arrowhead). This strengthens the notion that cells in the TF region rarely divide. Reduction in CycB was already apparent at 68 h AEL, prior to entry into third instar (Fig. 1F). At this stage, neither *hh-lacZ* nor En-positive cells were observed. Therefore, lack of CycB is currently our earliest marker for TF differentiation. As cells in the TF region have not yet acquired any known TF cell markers, but differ from anterior proliferating precursors, we term them TF precursors.

Activin signaling promotes somatic cell proliferation and increases gonad size

To find pathways that might affect TF precursor accumulation, we conducted an RNAi screen in larval ovaries using the driver *traffic jam* (*tj*)-Gal4, which is expressed in the somatic cells of the ovary but not in germ cells (Li et al., 2003). Four different RNAi constructs directed against the Activin receptor and three that are directed against its effector Smox produced markedly smaller gonads at the end of larval development (Fig. 2A,B; supplementary material Table S1). This size reduction could not be ascribed to cell death (supplementary material Table S2). Conversely, somatic overexpression of the activated Activin receptor ($Babo^{QD}$) resulted in a marked increase in gonad size (Fig. 2C; supplementary material Table S1). Similar results were obtained with the somatic driver *c587*-Gal4 (supplementary material Fig. S1). Activin signaling affected ovary size even prior to TF formation, as both total ovary size and that of the TF precursor region were affected prior to ML3 (Fig. 2D-I; supplementary material Tables S3, S4).

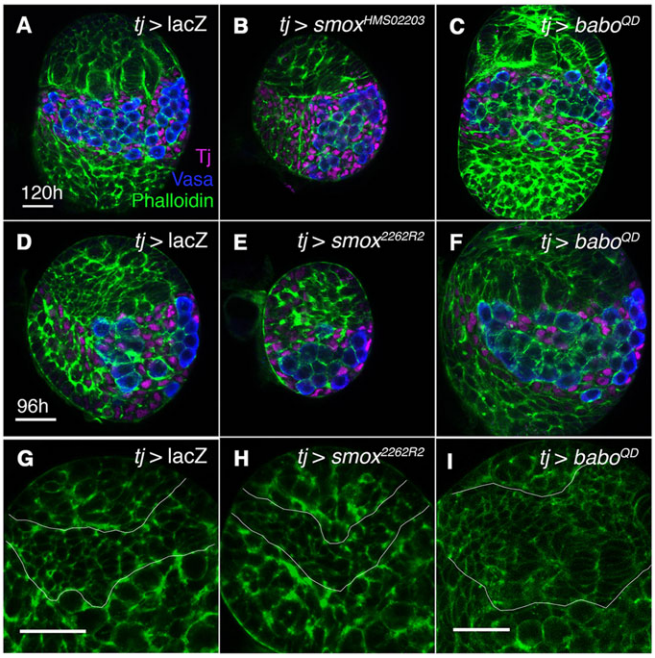

Fig. 2. Activin signaling increases gonad size. In all images, Alexa 488-phalloidin (green) outlines cell membranes. (A-F) Anti-Vasa (blue) marks germ cells and anti-Tj (magenta) marks ICs. (A-C) Gonads at 120 h AEL. Removal of somatic *Smox* results in smaller gonads (B), as compared with WT (A). Expression of $Babo^{QD}$ results in larger gonads (C). (D-F) Similar tendencies are observed at 96 h AEL. (G-I) TF precursor region (between white lines) is smaller in *Smox*-RNAi (H) and larger in $Babo^{QD}$ (I), as compared with WT (G). Ovary numbers are specified in supplementary material Tables S1-S4. Scale bars: 20 µm (in A for A-C; in D for D-F; in G for G,H; and in I).

Activin signaling affected cell proliferation, as *Smox*-RNAi ovaries contained fewer pH3-positive cells, even after correcting for the reduced gonad size (supplementary material Table S3). Interestingly, we could not detect a corresponding increase in cell proliferation upon $Babo^{QD}$ expression (supplementary material Table S5). A similar effect of Babo on imaginal disc size (a change of 20-30%), without detectable changes in the fraction of dividing cells, was previously reported (Brummel et al., 1999), suggesting that the effects of Activin on the cell cycle in some organs might be evenly distributed among the different cell cycle phases.

To analyze the effect of Activin on cell size, we measured both anterior cells and intermingled cells (ICs) and found that cell size changed little in *Smox*-RNAi or $Babo^{QD}$ ovaries (supplementary material Table S6). Cell proliferation and cell growth could be regulated either independently or by the same signals (Johnston and Gallant, 2002; Jorgensen and Tyers, 2004; Potter and Xu, 2001). Had cell growth been completely unaffected by Activin signaling, cells in *Smox*-RNAi ovaries, which divide less often, would have continued growing and would have been larger. However, cell size changed only slightly upon modulating Activin signaling, suggesting that it promotes both cell proliferation and growth.

Activin signaling promotes TF formation and PGC differentiation

In addition to increasing precursor cell proliferation/growth, Activin signaling promoted niche differentiation. At ML3, when TFs begin to form, a significant increase in TF stack numbers was observed in $Babo^{QD}$ ovaries as compared with WT (Fig. 3A,B,H; supplementary material Table S7). At 101 h AEL, these stacks were not only more numerous, but also longer (Fig. 3C,D,H; supplementary material Table S7). Thus, once TFs start forming, increased Activin signaling accelerates the process. By 120 h AEL, the anterior region of $Babo^{QD}$ ovaries contained TFs that were unevenly spaced (Fig. 3F, arrowheads, compare with 3E). This phenotype is reminiscent of *EcR*-RNAi and *usp*-RNAi ovaries, in which derepression of ecdysone target genes accelerates TF formation and results in uneven spacing of TFs (Gancz et al., 2011). The final TF number in $Babo^{QD}$ ovaries did not significantly differ from that of control ovaries (Fig. 3H; supplementary material Table S7); by the end of larval development (120 h AEL), the correct, adult numbers of TF stacks had already formed (Fig. 3H; supplementary material Table S7). By contrast, *Smox*-RNAi and *babo*-RNAi ovaries had fewer, shorter, TF stacks at 120 h AEL (Fig. 3G,H; supplementary material Table S7). Importantly, unlike WT, TFs in *Smox*-RNAi and *babo*-RNAi ovaries continued forming in the pupa, and ovariole numbers in the adult were higher than at 120 h (Fig. 3H; supplementary material Table S7). Thus, some mechanism allows a partial rescue of ovariole numbers following modulation of Activin signaling.

We have previously shown that, in some cases, TF differentiation is co-regulated with PGC differentiation (Gancz and Gilboa, 2013b; Gancz et al., 2011). Since Activin signaling promoted niche development, we tested its effects on PGC differentiation. At late third instar, PGCs that are located away from the niche lose BMP signaling and upregulate the major differentiation gene *bag of marbles* (*bam*). This developmental step can be monitored by the *bamP*-GFP reporter (Chen and McKearin, 2003; Zhu and Xie, 2003) (Fig. 4A). Reduction of somatic *Smox* by RNAi reduced *bamP*-GFP expression only marginally (Fig. 4B-D). However, *babo* reduction by four different RNAi constructs did result in a significant decrease in *bamP*-GFP levels (Fig. 4E-I). Conversely, $Babo^{QD}$ expression greatly enhanced PGC differentiation in a non-

Development (2015) 142, 883-892 doi:10.1242/dev.113902

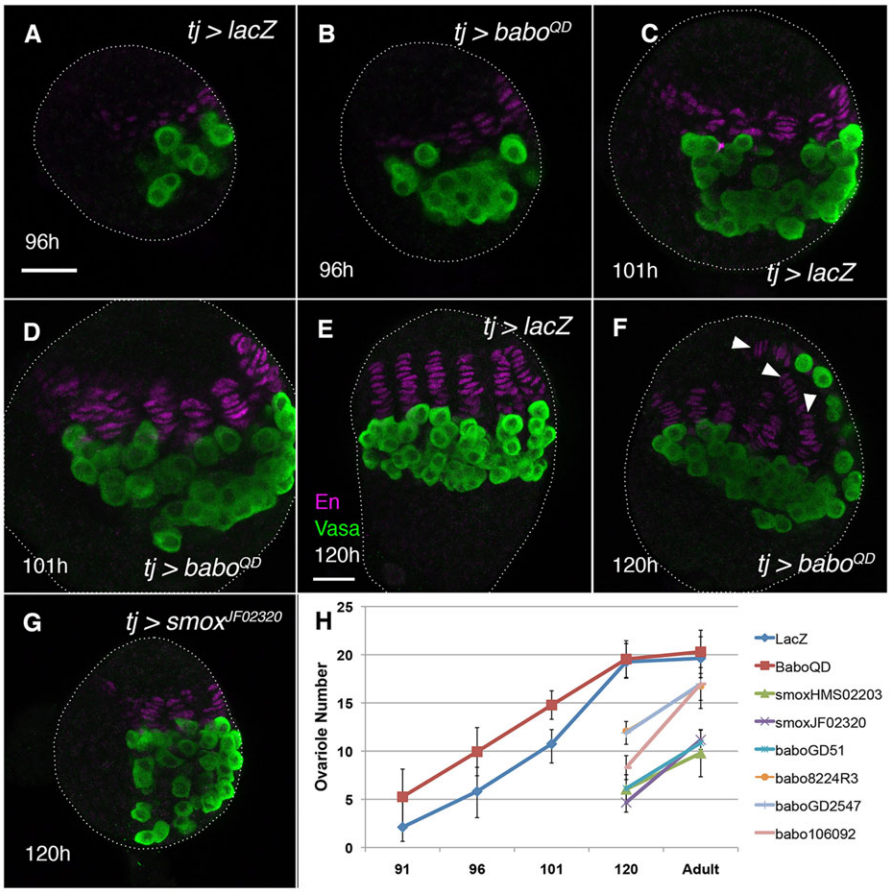

Fig. 3. Activin signaling promotes TF formation. In all images, anti-En (magenta) marks TF cells and anti-Vasa labels PGCs (green). Each image is a maximum intensity projection of six consecutive *z*-stacks through a region with the greatest concentration of TFs. (A,B) Gonads at 96 h AEL. Few TF cells are observed in WT (A). Babo^{QD} ovaries contain a few extra TFs (B). (C,D) Gonads at 101 h AEL. Increased numbers and taller stacks are observed in Babo^{QD} ovaries (D), as compared with WT (C). (E-G) Gonads at 120 h AEL. (E) In WT ovaries TF stacks are fully formed and normally spaced. (F) In Babo^{QD} gonads, faster TF formation leads to unevenly spaced TFs (arrowheads). (G) Removal of somatic *Smox* results in fewer, shorter stacks. (H) Quantification of niche numbers (*y*-axis) at various developmental times (*x*-axis, h AEL). *n* and *P*-values are provided in supplementary material Table S7. Error bars indicate s.d. Scale bars: 20 µm (in A for A-D; in E for E-G).

autonomous manner. As noted previously, at 96 h AEL, PGCs in WT ovaries are still proliferating and do not express *bamP*-GFP (Fig. 4J) (Gancz et al., 2011). By contrast, Babo^{QD}-overexpressing ovaries were filled with GFP-expressing PGCs, indicating that PGCs initiate their differentiation precociously (Fig. 4K). pMad labeling in PGCs that are close to niches remained normal in *Smox*-RNAi, *babo*-RNAi and Babo^{QD} ovaries, suggesting that BMP signaling could still maintain the prospective GSCs (supplementary material Fig. S2).

Precocious germline cyst formation was also observed following Babo^{QD} expression. We monitored cyst formation by the morphology of the fusome, an intracellular organelle within germ cells. Fusomes are round in PGCs, GSCs and their immediate daughter cells but branched in differentiating cysts (de Cuevas and Spradling, 1998). At 120 h AEL, WT *bam*-expressing PGCs still harbored a spherical fusome, indicating that cyst development has not yet occurred (Fig. 4L,M, arrowheads). By contrast, branched fusomes were prevalent in Babo^{QD} ovaries, showing that cyst development was underway (Fig. 4N,O, arrowheads). Combined, these data suggest that Activin signaling promotes both niche and PGC differentiation.

Ovarian Activin signaling does not affect EcR expression

Co-development of ovarian niches and PGCs is controlled by ecdysone signaling (Gancz et al., 2011). We therefore examined a possible association between the ovarian Activin and ecdysone pathways. In larval brains, Activin signaling has been shown to control the response to ecdysone by promoting the expression of the ecdysone receptor EcR-B1 (Yu et al., 2013; Zheng et al., 2003). However, whereas EcR-B1 expression in γ-neurons is developmentally regulated, ovarian EcR is continually expressed throughout third instar (Gancz et al., 2011). Indeed, staining with an antibody directed against EcR-B1 did not reveal a significant change in the expression of this isoform when either one of the three *Smox*-RNAi or four *babo*-RNAi constructs was expressed in the somatic cells of larval ovaries (Fig. 5A-H). Likewise, anti-EcR-A and anti EcR-C staining – directed against the A isoform and the common region of EcR, respectively – was not significantly changed (supplementary material Figs S3 and S4). Thus, ecdysone receptor expression in larval ovaries does not positively correlate with the status of Activin signaling.

To further explore a possible connection between the ecdysone and Activin pathways, we measured the effects of Activin on the transcription of various ecdysone target genes. *ftz-f1* and *Eip74EF* expression changed only a little (Fig. 5I). The *Eip75B* mRNA level was significantly increased in Babo^{QD} ovaries (Fig. 5I). However, only one *Smox*-RNAi construct resulted in a significant reduction of *Eip75B* mRNA levels (Fig. 5I). Thus, *Eip75B* might be somewhat affected by Activin signaling.

Our previous studies showed that the ecdysone target *broad* promotes niche and PGC differentiation and that the Br-Z1 isoform is specifically upregulated by ecdysone at the appropriate time (Gancz et al., 2011). Indeed, a consistent effect of Activin on *br-Z1* transcription was observed in larval ovaries; expression of Babo^{QD} increased *br-Z1* levels, whereas all three *Smox*-RNAi constructs reduced its levels significantly (Fig. 5J). By contrast, *br-Z2* did not respond strongly to changes in Activin signaling (Fig. 5K). *br-Z4* expression was significantly elevated by Babo^{QD} expression, but

Development (2015) 142, 883-892 doi:10.1242/dev.113902

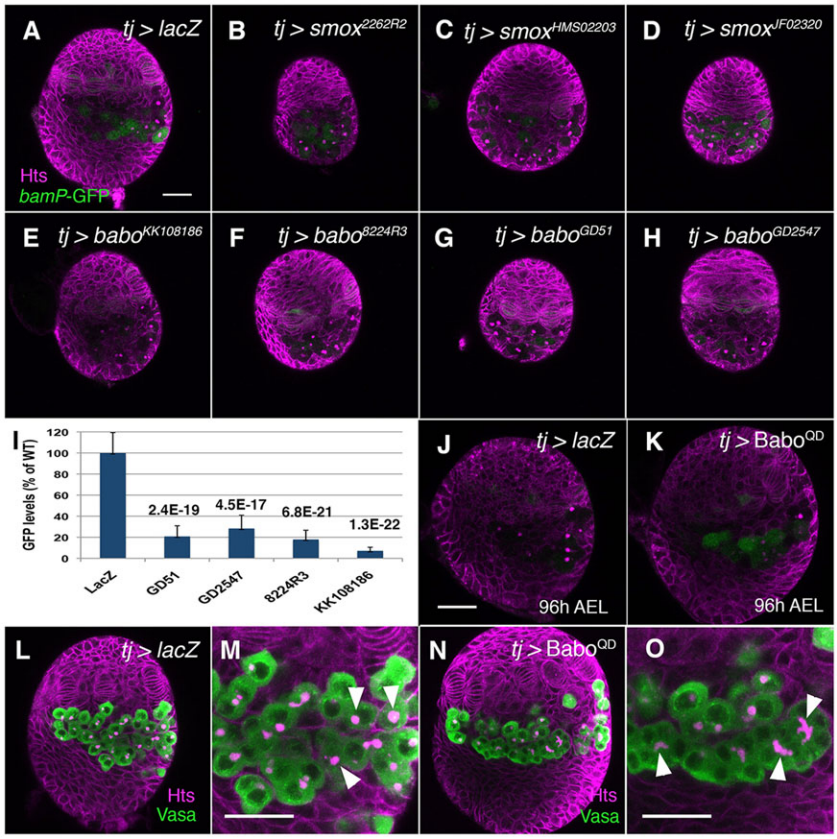

Fig. 4. Somatic Activin signaling promotes PGC differentiation. In all images, anti-Hts antibody (magenta) marks somatic cell cortices and fusomes within PGCs. (A-H,J,K) *bamP*-GFP (green) marks differentiating PGCs. (A) In WT ovaries at 120 h AEL, PGCs away from TFs upregulate *bam* and express GFP (n=24). (B-D) Removing *Smox* by RNAi reduces *bam*-GFP only slightly (n=16, 23, 19 for $Smox^{2262R2}$, $Smox^{HMS02203}$, $Smox^{JF02320}$, respectively). (E-H) Removal of somatic *babo* results in a significant decrease in GFP levels at 120 h AEL (n=22, 20, 20, 21, 19 ovaries, respectively). (I) Quantification of GFP levels (*bam*-GFP) in *babo*-RNAi ovaries. The different RNAi constructs and *t*-test *P*-values are specified. Values of control *lacZ* ovaries are set as 100%. Error bars indicate s.d. (J,K) Ovaries at 96 h AEL. (J) PGCs in WT ovaries (n=40) do not express *bamP*-GFP. (K) $Babo^{QD}$-overexpressing ovaries are filled with differentiating, GFP-positive PGCs (n=41). (L-O) PGCs are marked by anti-Vasa (green). (M,O) Enlargements of PGC region of L,N, respectively; they are composed of several compressed *z*-sections to allow better appreciation of fusome morphology. (L,M) Spherical fusomes in WT (M, arrowheads) indicate no cyst development (n=50). (N,O) Branched fusomes in $Babo^{QD}$ ovaries (O, arrowheads) indicate precocious cyst development (n=83). Scale bars: 20 µm (in A for A-H,L,N; in J for J,K; and in M,O).

was only slightly affected by *Smox*-RNAi, suggesting that it might not constitute a major target of Activin in the gonad.

The specific effects of Activin on only some ecdysone targets indicate that, in the ovary, Activin does not interact with the ecdysone pathway at the receptor level, but at the level of specific target genes. The consistent effect that we observed on Br-Z1, which is the same isoform that is upregulated by ecdysone, suggests that at least part of the effects of Activin on the ovary occur by controlling Br-Z1.

Activin signaling is required for Br-Z1 accumulation

To determine the effect of Activin signaling on Br-Z1 protein levels, we stained late third instar ovaries with anti-Br-Z1 antibody. At 120 h AEL, somatic nuclei of WT ovaries expressed high Br-Z1 levels (Fig. 6A,A′). Br-Z1 levels were even higher at 125 h AEL, in line with the high ecdysone levels at pupariation (Fig. 6B). By contrast, Br-Z1 levels were significantly lower in *Smox*-RNAi ovaries (Fig. 6C,C′). The reduction in Br-Z1 levels was stronger in ICs, which express Tj, and where the driver *tj*-Gal4 is strongly expressed. At the anterior of the gonad, where Tj and *tj*-Gal4 are expressed weakly, some Br-Z1 expression was observed (Fig. 6C′). Br-Z1 reduction in *Smox*-RNAi ovaries was less pronounced at pupariation, when high levels of ecdysone are present (compare Fig. 6D with 6B). Similar kinetics and localization of Br-Z1 expression were also observed in *babo*-RNAi ovaries (Fig. 6E-F).

To better quantify the modulation of Br-Z1 expression by Activin signaling, and to determine whether it acts in an autonomous or non-autonomous manner, we used mosaic analysis of the strong alleles $Smox^{MB388}$ and $babo^{32}$. Br-Z1 levels in mutant and neighboring WT cells were compared at specific time points during the last 24 h of larval development and at pupariation (Fig. 6G,H). For each time point, the percentage of clones showing 0-25%, 25-50%, 50-75% or >75% of WT Br-Z1 levels was calculated. The results show progressive Br-Z1 accumulation in both WT and mutant nuclei. However, Br-Z1 accumulated at a slower rate in mutant nuclei. These results are consistent with a role for Activin in enhancing Br-Z1 expression during the latter half of third instar.

To further test the idea of Br-Z1 modulation by Activin signaling, we analyzed its accumulation in ovaries expressing $Babo^{QD}$. At 91 h AEL, Br-Z1 was not observed in WT or $Babo^{QD}$ ovaries (Fig. 7A,B). Thus, activation of the pathway could not induce Br-Z1 expression prior to the timing specified by ecdysone signaling. At 96 h AEL, Br-Z1 is only beginning to be expressed in WT ovaries. However, its expression was clearly observed in $Babo^{QD}$ ovaries (Fig. 7C,D, arrowheads). Five hours later, at 101 h AEL, the elevation of Br-Z1 protein in $Babo^{QD}$ nuclei was still significant when compared with wild type (Fig. 7E,F). However, by 120 h AEL, when Br-Z1 was already strongly induced in all somatic WT nuclei, little difference was observed between control and $Babo^{QD}$ ovaries (Fig. 7G,H).

Combined, these results suggest that, as long as ecdysone receptors repress Br-Z1, Activin signaling cannot induce its expression. However, once Br-Z1 expression is induced by the hormone, the rate of its accumulation depends on Activin signaling.

Ecdysone-dependent and -independent functions of Activin signaling

If indeed Activin signaling cannot induce Br-Z1 expression independently of ecdysone signaling, then expression of the repressive dominant-negative EcRA.W650A form (EcR^{DN}) should be epistatic to $Babo^{QD}$ expression in the ovary. To test this, we co-expressed EcR^{DN} with either control *lacZ* or with $Babo^{QD}$. As expected of EcR^{DN} ovaries, no Br-Z1 was observed in Tj-expressing cells, even at 120 h AEL (Gancz et al., 2011). By contrast, cells at the anterior, which express low levels of *tj*-Gal4,

Development (2015) 142, 883-892 doi:10.1242/dev.113902

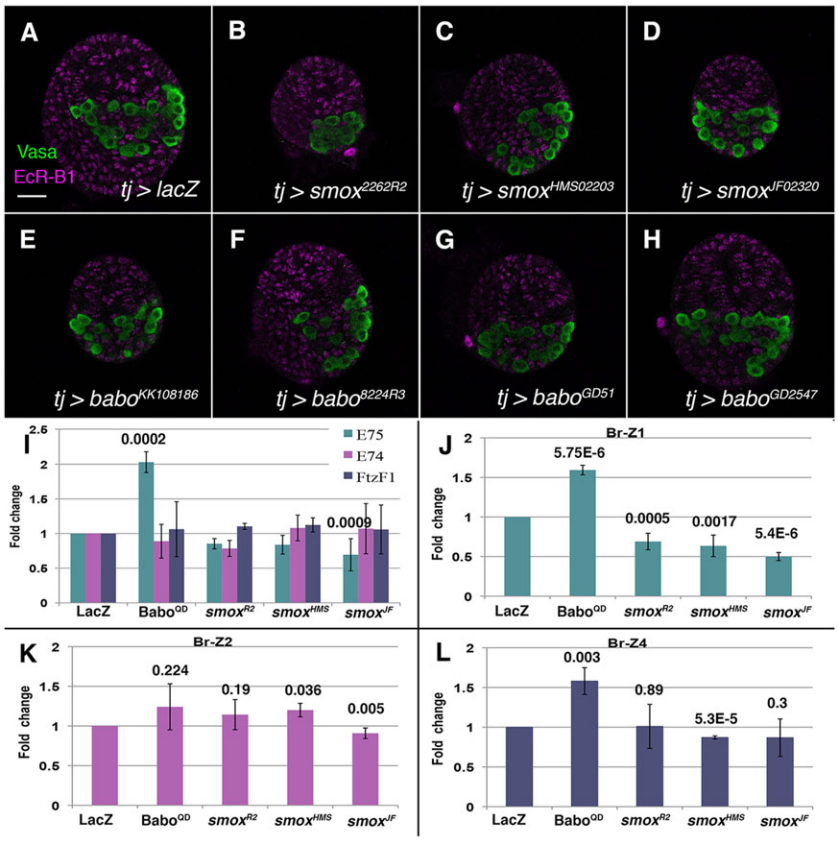

Fig. 5. Activin signaling promotes *br-Z1* transcription. (A-H) Somatic nuclei are marked by anti- EcR-B1 antibody (magenta); PGCs are stained with anti-Vasa (green). All somatic nuclei express similar levels of EcR-B1 in WT (A) and when somatic cells are devoid of *Smox* (B-D) or *babo* (E-H) (n>20 for each genotype). (I-L) Q-PCR of ecdysone target genes in ovaries that express $Babo^{QD}$ or *Smox*-RNAi. (I) *Eip75B* (E75), *Eip74EF* (E74) and *ftz-f1*; (J) *br-Z1*; (K) *br-Z2*; (L) *br-Z4*. *t*-test *P*-values are specified. Error bars indicate s.d. Scale bar: 20 µm (in A for A-H).

did express Br-Z1 (Fig. 8A,A′). Co-expression of $Babo^{QD}$ with EcR^{DN} did not result in Br-Z1 expression (Fig. 8B,B′).

Consistent with its inability to induce Br-Z1, $Babo^{QD}$ could not rescue PGC differentiation defects in EcR^{DN} ovaries. Whereas WT ovaries at prepupal stages exhibit germline cysts, indicating normal germ cell differentiation (Gancz and Gilboa, 2013b), no cysts were observed in either control EcR^{DN} or the experimental EcR^{DN}; $Babo^{QD}$ ovaries. In both cases only spherical fusomes were observed (Fig. 8C,D). Thus, activation of Activin signaling could not rescue Br-Z1 expression or the differentiation processes that associate with it.

Although $Babo^{QD}$ could not ameliorate the EcR^{DN}-induced block in differentiation, change was noted in gonad size. EcR^{DN}; $Babo^{QD}$ ovaries were distinctly larger than *lacZ*; EcR^{DN} ovaries (compare Fig. 8A with 8B, and 8C with 8D,E; supplementary material Table S8). This suggests that Activin promotes two separate activities: cell proliferation and cell differentiation. Cell differentiation is executed, at least in part, by controlling Br-Z1 accumulation downstream of ecdysone signaling. However, control of cell proliferation is independent of ecdysone signals and could be executed even in EcR^{DN}-expressing ovaries.

Consistent with this interpretation, removal of *broad* resulted in smaller ovaries (compare Fig. 8F with 8G) and additional removal of *babo* exacerbated the phenotype. Importantly, while little germ cell differentiation was observed in *babo*-RNAi ovaries (Fig. 4E-H), overexpression of Br-Z1 from a UAS promoter was sufficient to induce strong *bam* expression, as determined by *bam*-GFP levels (Fig. 8I). These results further strengthen the notion of Activin signaling having an ecdysone-dependent role in niche and PGC differentiation and an independent role in niche precursor proliferation.

DISCUSSION

We show that, during *Drosophila* ovarian formation, Activin signaling determines precursor cell proliferation in an ecdysone-independent manner and TF and PGC differentiation through modulating Br-Z1 accumulation. This coordination of the rates of cell proliferation and differentiation forms the basis of a correction mechanism for niche numbers.

A working model for ovarian niche differentiation

We show that cells with reduced proliferation capacity already appear at 68 h AEL, prior to entry into third instar (Fig. 1F). The exact time at which TF precursors first arise is unclear, since at earlier time points (48 h AEL) the small gonad size did not allow us to distinguish between a random group of cells that happen to be in G1/S phase and the clear linear structure of CycB-negative cells observed at 68 h AEL. The identification of a positive marker for TF precursors would help to resolve this issue.

Our observations also indicate that between 68 h and 96 h AEL the region of cuboidal cells that are devoid of CycB increases significantly. This corroborates a previous pulse-chase study that indicated a first wave of proliferation at 68-72 h AEL, in which BrdU-retaining somatic cells contributed ∼50% of all TF cells throughout the larval ovary. A second wave of proliferation during third instar occurred gradually and resulted in labeled TF cells that appeared from the medial to the lateral side of the ovary (Sahut-Barnola et al., 1996), matching the topology of mature filament appearance (Gancz et al., 2011; Godt and Laski, 1995; Hodin and Riddiford, 1998; Sahut-Barnola et al., 1996, 1995).

Combined, these studies suggest a sequence of events in which somatic precursors continually proliferate, giving rise to non- or rarely dividing box-shaped TF precursors as early as second instar.

Development (2015) 142, 883-892 doi:10.1242/dev.113902

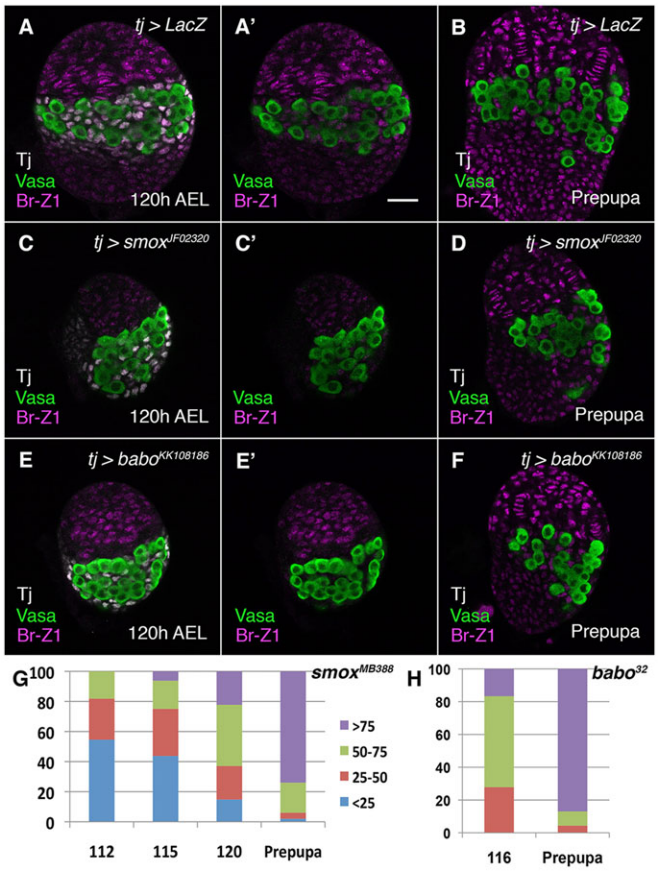

Fig. 6. Reduced Activin signaling attenuates the accumulation rate of Br-Z1. (A-F) Br-Z1 is magenta, PGCs are green (anti-Vasa), somatic ICs are in white (anti-Tj). (A-B) Control ovaries. (A,A′) Br-Z1 is expressed in all somatic nuclei at 120 h AEL (n=31). (B) Expression is stronger during pupariation (n=26). (C-D) Lower Br-Z1 levels are observed in *Smox*-RNAi ovaries (n=30). (D) In the prepupa, some recovery of Br-Z1 expression is noted (n=23). (E-F) A similar pattern of Br-Z1 reduction is seen in *babo*-RNAi ovaries (n=29 larval and n=13 prepupal ovaries). (G) Quantification of Br-Z1 expression in $Smox^{MB388}$ clones at 112 h, 115 h, 120 h AEL and prepupa (n=22, 32, 27 and 50 clones, respectively). Clones were divided into bins according to Br-Z1 levels that were below 25%, 25-50%, 50-75% or >75% of WT levels. (H) Quantification of Br-Z1 expression in $babo^{32}$ mutant clones at 116 h AEL and prepupa (n=18 and n=23 clones, respectively). Scale bar: 20 µm (in A′ for A-F).

TF precursors continue to accumulate through early third instar. During the latter half of third instar, TF precursors express TF markers such as En and *hh-lacZ*, organize into filaments and attain the mature disc shape of terminally differentiated TF cells (Fig. 8J). We term the proliferating cells somatic precursors, rather than TF precursors, since they give rise to more than the TF lineage (Sahut-Barnola et al., 1996). We reserve the term TF precursors for the non-proliferating cells that give rise only to mature TF cells. Further understanding of the lineage awaits the identification of additional markers and TF determinants.

Correction of niche numbers through balancing proliferation and differentiation

The sequence of events leading to TF differentiation suggests that niche numbers could be determined by the rate of somatic precursor cell proliferation, which affects the pool size from which TF precursors are drawn. Insulin signaling, which greatly increases ovarian cell numbers, acts at this level (Gancz and Gilboa, 2013b). A second factor is the timing of TF precursor cell differentiation. Once a cell becomes a TF precursor, it effectively reduces the pool of cells that could proliferate to give rise to more TF cells in the future. We have previously shown that Br-Z1 overexpression and precocious expression results in smaller gonads with fewer TFs (Gancz et al., 2011). This fits a model in which the proliferating pool size is decreased by precocious differentiation and removal of cells from the mitotic to the non-mitotic pool.

We now show that the rate of Br-Z1 accumulation in somatic nuclei can be modulated by Activin signaling (Figs 6 and 7). Three lines of evidence suggest that the differentiation function of Activin depends on modulating the ecdysone response. First, we show that Br-Z1, which is a major target of the ecdysone pathway, is also a target of the Activin pathway. Second, only after induction of Br-Z1 by ecdysone can $Babo^{QD}$ increase Br-Z1 accumulation. Third, we show that ecdysone is epistatic to Activin function in promoting Br-Z1 expression, as well as niche and PGC differentiation (Fig. 8).

Importantly, Activin signaling also controls ovarian cell proliferation. Our epistasis analysis suggests that, unlike its role in niche differentiation, Activin promotes proliferation in an ecdysone-independent fashion. This places Activin signaling as an important balancer of proliferation and differentiation. Upon activation of the pathway, increased somatic precursor cell proliferation enlarges the pool of TF precursors. However, the rate of TF cell differentiation is also increased. This removes more cells from the effective proliferating population, resulting in normal niche numbers (Fig. 8K). Conversely, when Activin signaling is reduced, cell proliferation diminishes and the precursor pool is smaller. To balance this, the rate of TF differentiation is also reduced. This allows the slowly proliferating precursors additional time to increase their numbers

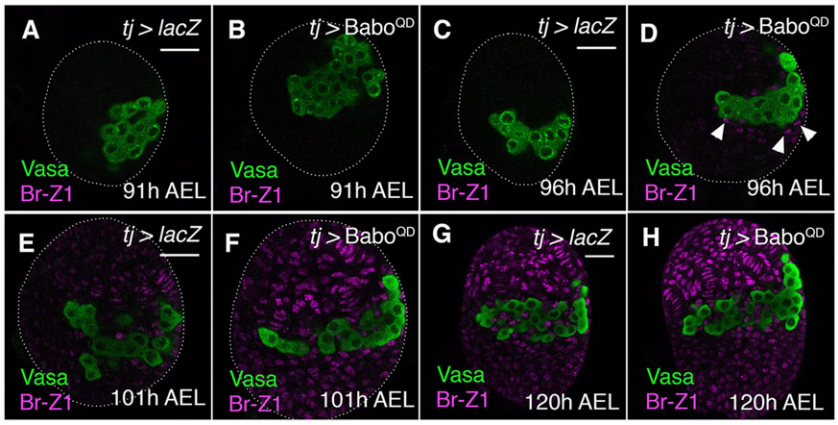

Fig. 7. Increased Activin signaling promotes Br-Z1 accumulation. In all images, Br-Z1 is magenta, PGCs are green (anti-Vasa). (A,B) At 91 h AEL, no Br-Z1 staining is seen in WT (A) or $Babo^{QD}$ (B) ovaries (n=7 and n=9, respectively). (C,D) At 96 h AEL, very low levels of Br-Z1 are detected in WT (C), whereas Br-Z1 is easily observed (arrowheads) in $Babo^{QD}$ ovaries (D) (n=19 and n=22, respectively). (E,F) At 101 h AEL, Br-Z1 is easily observed in WT ovaries (E), although levels are higher in $Babo^{QD}$ ovaries (F) (n=13 and n=11, respectively). (G,H) At 120 h AEL, levels of Br-Z1 are similar in WT (G) and $Babo^{QD}$ (H) ovaries (n=25 and n=30, respectively). Scale bars: 20 µm (in A for A,B; in C for C,D; in E for E,F; in G for G,H).

Development (2015) 142, 883-892 doi:10.1242/dev.113902

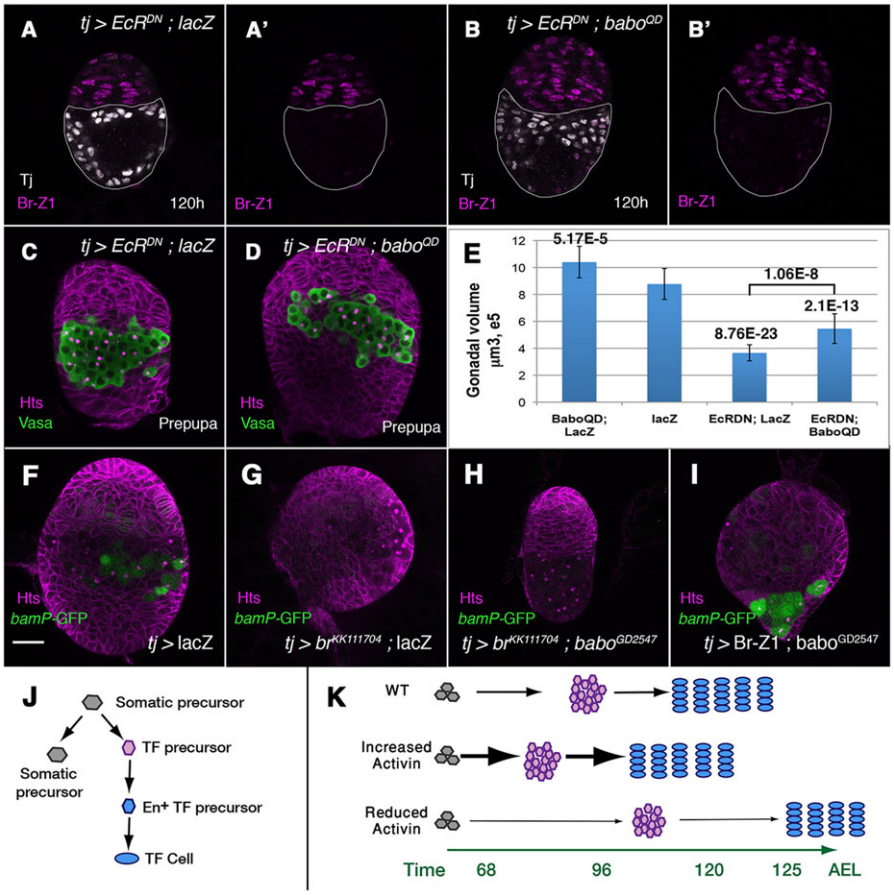

Fig. 8. Ecdysone-dependent and -independent roles of Activin signaling. (A-B′) Ovaries at 120 h AEL; Br-Z1 is in magenta, Tj is in white. (A,A′) Reduced size of EcR^{DN} ovaries. Br-Z1 is not expressed in most Tj-positive cells (white line in A′) (*n*=30). (B,B′) Co expression of EcR^{DN} with $Babo^{QD}$. Most somatic nuclei that are TJ positive are still devoid of Br-Z1 (within white line in B′). Ovaries are larger than in A (*n*=23). (C,D) Prepupal ovaries, somatic cells and fusomes within germ cells are marked by anti-Hts (magenta) and PGCs by anti-Vasa (green). Gonads co-expressing EcR^{DN} with $Babo^{QD}$ (D; *n*=24) are larger than those expressing EcR^{DN} with *lacZ* (C; *n*=28); however, spherical fusomes within PGCs indicate that cysts fail to develop. (E) Quantification of gonad volumes. The different genotypes and *t*-test *P*-values are marked. Error bars indicate s.d. (F-I) PGC differentiation is marked by *bamP*-GFP (anti-GFP, green). *broad*-RNAi (G; *n*=10) ovaries are smaller than WT (F; *n*=26) and do not express GFP. Additional removal of *babo* results in even smaller ovaries (compare G with H; *n*=12). (I) Overexpression of Broad in *babo*-RNAi ovaries rescues germ cell differentiation (green) (*n*=22). (J) Model of TF differentiation. Proliferating somatic precursors produce non- or rarely proliferating TF precursors that sequentially change their shape, acquire adult TF markers and stack in filaments. See Discussion for details. (K) Model showing how Activin signaling determines niche numbers. Activin controls somatic precursor proliferation (gray cells) and thus determines TF precursor numbers (pink cells). Activin also determines the rate of TF cell differentiation (blue cells). See Discussion for details. Arrow thickness represents signal strength. Scale bar: 20 µm (in F for A-D,F-I).

prior to TF differentiation. Collectively, ecdysone signaling, which controls the major switch from proliferation to differentiation, and Activin signaling, which fine-tunes these processes, demonstrate how co-regulation of cell proliferation and differentiation may be used to adjust niche numbers during development.

Control of PGC differentiation via somatic signaling

We have previously shown that Broad is an essential target for the ovarian ecdysone response, which includes niche and PGC differentiation (Gancz et al., 2011). However, other ecdysone targets might also participate in niche/PGC differentiation. We now show that both Br-Z1 accumulation and TF formation are slower in *Smox*-RNAi and *babo*-RNAi ovaries. Interestingly, *bamP*-GFP, which is indicative of PGC differentiation, accumulates almost normally in *Smox*-RNAi but not in *babo*-RNAi ovaries (Fig. 4). Since Br-Z1 levels are reduced in both *Smox*-RNAi and *babo*-RNAi ovaries, an exciting possibility is that additional ecdysone targets are involved in the somatic control of PGC differentiation. What these targets might be is currently unknown. Moreover, the fact that PGCs fail to differentiate when the Activin receptors are reduced but not when the downstream effector is knocked down suggests that at least part of the function of Activin in the ovary might be *Smox* independent (Derynck and Zhang, 2003; Moustakas and Heldin, 2005; Ng, 2008; Ozdamar et al., 2005). If so, how such targets induce PGC differentiation remains to be investigated. Our analysis of Activin ligands suggests that activation of the pathway is mostly, if not entirely, dependent on somatically produced ligands (supplementary material Table S1). The Activin pathway therefore provides another example of how the ovarian soma controls germline differentiation.

Different modes of interaction between the ecdysone and Activin pathways

The Activin and ecdysone pathways have previously been shown to associate in the nervous system and in the prothoracic gland (Gibbens et al., 2011; Zheng et al., 2003, 2006). Interestingly, in

Development (2015) 142, 883-892 doi:10.1242/dev.113902

each case, the Activin pathway serves to potentiate the function of ecdysone, and in each case Activin affects the ecdysone response at a different level. In the prothoracic gland, Activin is required for the expression of receptors for Prothoracicotropic hormone and Insulin, which control the expression of several ecdysone biosynthetic enzymes. It is thus placed upstream of the ecdysone response (Gibbens et al., 2011). In mushroom body γ neurons, Activin potentiates axonal pruning by promoting the expression of EcR-B1 (Zheng et al., 2003). A similar molecular function for Activin was identified in dorsal cluster neurons, where it was suggested that Activin is required to modulate the rate of neuronal terminal differentiation (Zheng et al., 2006).

In the ovary, Activin interacts with the ecdysone pathway at the level of the target gene *br-Z1*. Unlike in the nervous system, the ecdysone receptor is continually expressed in larval ovaries, since it fulfills the dual role of an early repressor and a late activator of stem cell unit differentiation (Gancz et al., 2011). This explains why the phenotypes of Babo^{QD} overexpression in larval ovaries are similar to *EcR*-RNAi phenotypes (Gancz et al., 2011); in both cases, *br-Z1* is upregulated. Since ecdysone receptors are required as early repressors and late activators of Br-Z1 expression and GSC unit differentiation, there is more logic in placing a potentiator of the pathway at the level of the target gene and not the receptor. How the two pathways were connected at different nodes in different tissues during evolution remains an open question.

MATERIALS AND METHODS

Fly stocks

The following stocks were from the Bloomington Stock Center: Oregon Red (OR), *UAS*-EcRA.W650A (EcR^{DN}), FRT19A, *arm-lacZ*, *Smox*^{MB388}, *babo*^{32}, and RNAi lines directed against *Smox* (HMS02203, JF02320). From the Vienna Drosophila RNAi Center (VDRC): RNAi lines against *babo* (KK108186, GD51, GD2547). From NIF-Fly: RNAi line against *babo* (8224R3) and against *Smox* (2262R2). From the Drosophila Genetic Resource Center: *tj*-Gal4 (P{GawB}NP1624). *bamP*-GFP located on the X chromosome was obtained from Dr Dennis McKearin (HHMI). *UAS-lacZ* was provided by Dr Jessica Treisman (NYU School of Medicine, USA). UAS-Babo^{QD} was from Dr Theodor Haerry. *c587*-Gal4 was from Prof. Ting Xie (Stowers Institute, USA). *Smox*^{MB388} clones were generated using the line *hs*-Flp^{122}, FRT19A, *arm-lacZ* and induced by heat shock at 48 h AEL for 35 min at 37°C. *babo*^{32} clones were generated using the line *c587*-Gal4, *UAS*-flp; FRT42D.

Larval staging

To obtain flies at similar developmental stages, care was taken to work with undercrowded cultures. Flies were transferred into fresh bottles (rather than vials) to lay eggs for 2 hours, and were then removed. Bottles were left at 25°C for 68-125 h; 68 h (late second instar), 96 h (mid-larval third instar), 120 h (late larval third instar) and 125 h (prepupa). Under these conditions the development of WT gonads is uniform. The terminology we use is according to Ashburner et al. (2005).

Antibody staining

The following monoclonal antibodies were obtained from the Developmental Studies Hybridoma Bank, developed under the auspices of the NICHD and maintained by the University of Iowa, Department of Biology: anti-Hts (1B1, developed by Dr Howard Lipshitz), 1:20; anti-Broad-Z1 (Z1.3C11.OA1, developed by Dr Greg Guild), 1:10; anti-Engrailed (4D9, developed by Dr Corey Goodman), 1:20; anti-EcRA (15G1a; 1:10), anti-EcRB1 (AD4.4; 1:10) and anti-EcRC (AG10.2; 1:10) developed by Drs Carl Thummel and David Hogness; anti-CycB (F2F4, developed by Dr O'Farrell), 1:15. Rabbit anti-Vasa (1:5000) was a gift from Dr Ruth Lehmann (HHMI, New York University). Guinea pig anti-Tj (1:7000) was a gift from Dr Dorothea Godt (University of Toronto). Rabbit anti-β-galactosidase (β-gal) (1:15,000) was from Cappel (08559762). Rabbit anti-GFP (1:1000) was from Invitrogen (A11122). Rabbit anti-phospho-Histone H3 (1:1000) was from Millipore (06-570). Alexa 488-phalloidin was from Life Technologies. Secondary antibodies were from Jackson ImmunoResearch or from Invitrogen and used according to the manufacturer's specifications. The staining protocol was as previously described (Gancz et al., 2011).

EdU (Invitrogen, C10337) was used to label cells in S phase, propidium iodide (Sigma, P4864) to label dead cells and DAPI to label nuclei of adult ovaries, all according to the manufacturer's specifications.

Imaging

Confocal imaging was with a Zeiss LSM 710 on a Zeiss Observer Z1. For analysis of *bamP*-GFP, GFP-positive PGCs located at the mid-section of an ovary were marked and the Measure tool in ImageJ (NIH) was applied. For Broad-Z1 staining intensity in *Smox*^{MB388} and *babo*^{32} clones, the middle sections of a mutant and an adjacent WT cell were chosen and the Measure tool used for the selected cell area. For cell size and the size of the TF precursor region, the Measure tool was also used. For ovary volume, the Surface tool in Imaris software (Bitplane) was used.

Real-time PCR

15-20 ovaries were collected from early L3 larvae (112 h AEL). Tissue was disrupted using QIAshredder (Qiagen) and RNA isolated using the RNeasy Kit (Qiagen) according to the manufacturer's instructions. Reverse transcription was performed with the High Capacity cDNA Reverse Transcription Kit (Applied Biosystems). Q-PCR employed SYBR Green (Invitrogen) with the following primers (forward and reverse): CAAGATTGCCGGCTATGTCA and CCTGCAACTTGATGGAGATA-CCA for *RpS17*; ACAATCCGCACCACAGAAAC and GCCGGAACTG-GAGCTGTC for *Eip74EF*; CTCCTACTCCATGCCCACAC and GCTGC-GAGAACTCCTGCT for *Eip75B*; AGTAGACTGGGCACG-GAACA and CAGGTGATCCAGAACAAGCA for *ftz-f1* (all from Sigma-Aldrich); or TaqMan assays: *RpL32* (Dm02151827), *br-Z1* (Dm01837161_m1), *br-Z2* (Dm01821011_m1), *br-Z4* (Dm01821-013_m1).

Q-PCR was performed in a StepOne real-time PCR system (Applied Biosystems) and analyzed by ΔΔCT and normalized to *RpS17* or *RpL32*.

Statistics

For statistical analyses, two-tailed Student's *t*-tests were performed. *P*-values are indicated.

Acknowledgements

We thank Drs Michael B. O'Connor and Theodor E. Haerry for generously providing fly stocks and Dr Dorothea Godt for anti-Tj antibodies.

Competing interests

The authors declare no competing or financial interests.

Author contributions

T.L., D.G. and L.G. designed and performed the experiments; L.G. wrote the manuscript.

Funding

This work was supported by the Israel Science Fund [grant number 1316/12]. L.G. is an incumbent of the Skirball Career Development Chair in New Scientists.

Supplementary material

Supplementary material available online at
http://dev.biologists.org/lookup/suppl/doi:10.1242/dev.113902/-/DC1

References

Ashburner, M., Golic, K. G. and Hawley, S. R. (2005). *Drosophila a Laboratory Handbook*. Cold Spring Harbor: Cold Spring Harbor Laboratory Press.

Bai, H., Kang, P., Hernandez, A. M. and Tatar, M. (2013). Activin signaling targeted by insulin/dFOXO regulates aging and muscle proteostasis in Drosophila. *PLoS Genet.* **9**, e1003941.

Bartoletti, M., Rubin, T., Chalvet, F., Netter, S., Dos Santos, N., Poisot, E., Paces-Fessy, M., Cumenal, D., Peronnet, F., Pret, A.-M. et al. (2012). Genetic

basis for developmental homeostasis of germline stem cell niche number: a network of Tramtrack-Group nuclear BTB factors. *PLoS ONE* **7**, e49958.
Bayer, C. A., Holley, B. and Fristrom, J. W. (1996). A switch in broad-complex zinc-finger isoform expression is regulated posttranscriptionally during the metamorphosis of Drosophila imaginal discs. *Dev. Biol.* **177**, 1-14.
Bolívar, J., Pearson, J., López-Onieva, L. and González-Reyes, A. (2006). Genetic dissection of a stem cell niche: the case of the Drosophila ovary. *Dev. Dyn.* **235**, 2969-2979.
Brummel, T., Abdollah, S., Haerry, T. E., Shimell, M. J., Merriam, J., Raftery, L., Wrana, J. L. and O'Connor, M. B. (1999). The Drosophila activin receptor baboon signals through dSmad2 and controls cell proliferation but not patterning during larval development. *Genes Dev.* **13**, 98-111.
Chao, A. T. and Guild, G. M. (1986). Molecular analysis of the ecdysterone-inducible 2B5 "early" puff in Drosophila melanogaster. *EMBO J.* **5**, 143-150.
Chen, D. and McKearin, D. M. (2003). A discrete transcriptional silencer in the bam gene determines asymmetric division of the Drosophila germline stem cell. *Development* **130**, 1159-1170.
Chen, S., Wang, S. and Xie, T. (2011). Restricting self-renewal signals within the stem cell niche: multiple levels of control. *Curr. Opin. Genet. Dev.* **21**, 684-689.
Clark, R. I., Woodcock, K. J., Geissmann, F., Trouillet, C. and Dionne, M. S. (2011). Multiple TGF-beta superfamily signals modulate the adult Drosophila immune response. *Curr. Biol.* **21**, 1672-1677.
de Cuevas, M. and Spradling, A. C. (1998). Morphogenesis of the Drosophila fusome and its implications for oocyte specification. *Development* **125**, 2781-2789.
Derynck, R. and Zhang, Y. E. (2003). Smad-dependent and Smad-independent pathways in TGF-beta family signalling. *Nature* **425**, 577-584.
DiBello, P. R., Withers, D. A., Bayer, C. A., Fristrom, J. W. and Guild, G. M. (1991). The Drosophila Broad-Complex encodes a family of related proteins containing zinc fingers. *Genetics* **129**, 385-397.
Eliazer, S. and Buszczak, M. (2011). Finding a niche: studies from the Drosophila ovary. *Stem Cell Res. Ther.* **2**, 45.
Ellis, J. E., Parker, L., Cho, J. and Arora, K. (2010). Activin signaling functions upstream of Gbb to regulate synaptic growth at the Drosophila neuromuscular junction. *Dev. Biol.* **342**, 121-133.
Gancz, D. and Gilboa, L. (2013a). Hormonal control of stem cell systems. *Annu. Rev. Cell Dev. Biol.* **29**, 137-162.
Gancz, D. and Gilboa, L. (2013b). Insulin and Target of rapamycin signaling orchestrate the development of ovarian niche-stem cell units in Drosophila. *Development* **140**, 4145-4154.
Gancz, D., Lengil, T. and Gilboa, L. (2011). Coordinated regulation of niche and stem cell precursors by hormonal signaling. *PLoS Biol.* **9**, e1001202.
Gibbens, Y. Y., Warren, J. T., Gilbert, L. I. and O'Connor, M. B. (2011). Neuroendocrine regulation of Drosophila metamorphosis requires TGFbeta/Activin signaling. *Development* **138**, 2693-2703.
Godt, D. and Laski, F. A. (1995). Mechanisms of cell rearrangement and cell recruitment in Drosophila ovary morphogenesis and the requirement of bric a brac. *Development* **121**, 173-187.
Green, D. A., II and Extavour, C. G. (2012). Convergent evolution of a reproductive trait through distinct developmental mechanisms in Drosophila. *Dev. Biol.* **372**, 120-130.
Green, D. A., II and Extavour, C. G. (2014). Insulin signalling underlies both plasticity and divergence of a reproductive trait in Drosophila. *Proc. R. Soc. B Biol. Sci.* **281**, 20132673.
Hodin, J. and Riddiford, L. M. (1998). The ecdysone receptor and ultraspiracle regulate the timing and progression of ovarian morphogenesis during Drosophila metamorphosis. *Dev. Genes Evol.* **208**, 304-317.
Johnston, L. A. and Gallant, P. (2002). Control of growth and organ size in Drosophila. *Bioessays* **24**, 54-64.
Jorgensen, P. and Tyers, M. (2004). How cells coordinate growth and division. *Curr. Biol.* **14**, R1014-R1027.
Karim, F. D., Guild, G. M. and Thummel, C. S. (1993). The Drosophila Broad-Complex plays a key role in controlling ecdysone-regulated gene expression at the onset of metamorphosis. *Development* **118**, 977-988.
König, A., Yatsenko, A. S., Weiss, M. and Shcherbata, H. R. (2011). Ecdysteroids affect Drosophila ovarian stem cell niche formation and early germline differentiation. *EMBO J.* **30**, 1549-1562.
Li, M. A., Alls, J. D., Avancini, R. M., Koo, K. and Godt, D. (2003). The large Maf factor Traffic Jam controls gonad morphogenesis in Drosophila. *Nat. Cell Biol.* **5**, 994-1000.
Losick, V. P., Morris, L. X., Fox, D. T. and Spradling, A. (2011). Drosophila stem cell niches: a decade of discovery suggests a unified view of stem cell regulation. *Dev. Cell* **21**, 159-171.
Massagué, J. (2012). TGFbeta signalling in context. *Nat. Rev. Mol. Cell Biol.* **13**, 616-630.
Miyazono, K., Ten Dijke, P. and Heldin, C.-H. (2000). TGF-beta signaling by Smad proteins. *Adv. Immunol.* **75**, 115-157.
Moustakas, A. and Heldin, C.-H. (2005). Non-Smad TGF-beta signals. *J. Cell Sci.* **118**, 3573-3584.
Ng, J. (2008). TGF-beta signals regulate axonal development through distinct Smad-independent mechanisms. *Development* **135**, 4025-4035.
Ozdamar, B., Bose, R., Barrios-Rodiles, M., Wang, H.-R., Zhang, Y. and Wrana, J. L. (2005). Regulation of the polarity protein Par6 by TGFbeta receptors controls epithelial cell plasticity. *Science* **307**, 1603-1609.
O'Brien, L. E. and Bilder, D. (2013). Beyond the niche: tissue-level coordination of stem cell dynamics. *Annu. Rev. Cell Dev. Biol.* **29**, 107-136.
Parker, L., Ellis, J. E., Nguyen, M. Q. and Arora, K. (2006). The divergent TGF-beta ligand Dawdle utilizes an activin pathway to influence axon guidance in Drosophila. *Development* **133**, 4981-4991.
Peterson, A. J. and O'Connor, M. B. (2013). Activin receptor inhibition by Smad2 regulates Drosophila wing disc patterning through BMP-response elements. *Development* **140**, 649-659.
Potter, C. J. and Xu, T. (2001). Mechanisms of size control. *Curr. Opin. Genet. Dev.* **11**, 279-286.
Sahut-Barnola, I., Godt, D., Laski, F. A. and Couderc, J.-L. (1995). Drosophila ovary morphogenesis: analysis of terminal filament formation and identification of a gene required for this process. *Dev. Biol.* **170**, 127-135.
Sahut-Barnola, I., Dastugue, B. and Couderc, J.-L. (1996). Terminal filament cell organization in the larval ovary of Drosophila melanogaster: ultrastructural observations and pattern of divisions. *Roux's Arch. Dev. Biol.* **205**, 356-363.
Sarikaya, D. P., Belay, A. A., Ahuja, A., Dorta, A., Green, D. A., II and Extavour, C. G. (2012). The roles of cell size and cell number in determining ovariole number in Drosophila. *Dev. Biol.* **363**, 279-289.
Song, X., Zhu, C.-H., Doan, C. and Xie, T. (2002). Germline stem cells anchored by adherens junctions in the Drosophila ovary niches. *Science* **296**, 1855-1857.
Song, X., Call, G. B., Kirilly, D. and Xie, T. (2007). Notch signaling controls germline stem cell niche formation in the Drosophila ovary. *Development* **134**, 1071-1080.
Spradling, A., Fuller, M. T., Braun, R. E. and Yoshida, S. (2011). Germline stem cells. *Cold Spring Harb. Perspect. Biol.* **3**, a002642.
Ting, C.-Y., McQueen, P. G., Pandya, N., Lin, T.-Y., Yang, M., Reddy, O. V., O'Connor, M. B., McAuliffe, M. and Lee, C.-H. (2014). Photoreceptor-derived activin promotes dendritic termination and restricts the receptive fields of first-order interneurons in Drosophila. *Neuron* **81**, 830-846.
Xie, T. and Spradling, A. C. (2000). A niche maintaining germ line stem cells in the Drosophila ovary. *Science* **290**, 328-330.
Yu, X. M., Gutman, I., Mosca, T. J., Iram, T., Özkan, E., Garcia, K. C., Luo, L. and Schuldiner, O. (2013). Plum, an immunoglobulin superfamily protein, regulates axon pruning by facilitating TGF-beta signaling. *Neuron* **78**, 456-468.
Zheng, X., Wang, J., Haerry, T. E., Wu, A. Y.-H., Martin, J., O'Connor, M. B., Lee, C.-H. J. and Lee, T. (2003). TGF-beta signaling activates steroid hormone receptor expression during neuronal remodeling in the Drosophila brain. *Cell* **112**, 303-315.
Zheng, X., Zugates, C. T., Lu, Z., Shi, L., Bai, J.-M. and Lee, T. (2006). Baboon/dSmad2 TGF-beta signaling is required during late larval stage for development of adult-specific neurons. *EMBO J.* **25**, 615-627.
Zhu, C.-H. and Xie, T. (2003). Clonal expansion of ovarian germline stem cells during niche formation in Drosophila. *Development* **130**, 2579-2588.
Zhu, C. C., Boone, J. Q., Jensen, P. A., Hanna, S., Podemski, L., Locke, J., Doe, C. Q. and O'Connor, M. B. (2008). Drosophila Activin- and the Activin-like product Dawdle function redundantly to regulate proliferation in the larval brain. *Development* **135**, 513-521.